www.sciencemag.org/cgi/content/full/313/5789/935/DC1

Supporting Online Material for

Pinwheels in the Quintuplet Cluster

Peter Tuthill,* John Monnier, Angelle Tanner, Donald Figer, Andrea Ghez, William Danchi

*To whom correspondence should be addressed. E-mail: p.tuthill@physics.usyd.edu.au

Published 18 August 2006, *Science* **313**, 935 (2006)
DOI: 10.1126/science.1128731

This PDF file includes:

Materials and Methods
Fig. S1
Table S1
References and Notes

1. Observations and Discussion

Observations of the Quintuplet cluster are listed in Table S1 and were made with the near-infrared NIRC camera on the Keck 1 telescope. The nomenclature of Moneti et al.(5) is adopted here, identifying the dusty red Quintuplet proper members, or cocoon stars, as Q 1, Q 2, Q 3, Q 4 and Q 9. Locations of each of these stars within the cluster as imaged by the Hubble Space Telescope is given in Fig. S1, which also depicts our diffraction-limited Keck images of Q 2, Q 3 overlayed with graphical indication of the relative spatial scale.

The high angular resolution imaging utilized rapid-exposure speckle interferometry techniques from a number of long-standing experiments at the Keck 1 (8). Typical datasets entailed from one to a few hundred short-exposures ($\sim$0.14 sec) with the NIRC camera operating in a high-magnification (0.0206 arcsec/pixel) mode. Interleaved observations of galactic-center object IRS 7 were used to calibrate the telescope-atmosphere point-spread function (the unresolved nature of this object was itself checked against stars HD 159255 and HD 163042).

All five Quintuplet cocoon stars were found to be spatially resolved to some degree. The full-width at half-maximum (FWHM) of best-fitting circular Gaussian functions, used here to give an estimate of apparent size, are given in Table S1. Images of stars Q 2 and Q 3, recovered with Fourier techniques(8) and presented earlier in Fig. 1, show that complex and asymmetric structures exist within the dust shells surrounding these stars. The complexity of these visibility functions resulted in poor fits for the Gaussian model, and we therefore limited the fit range to low spatial frequencies/short baselines where visibility excursions are not yet strongly manifest ($<2\times10^6$ and $1\times10^6\,\mathrm{rad}^{-1}$ for 2.21 and 3.08 μm respectively: equivalent to $\lesssim$4.5 and 3.1 m).

By implication, if similar physics is assumed to pertain to the remaining three of the five Quintuplet cocoon stars, then the utility of fitting Gaussian shells may appear limited. Despite this, for objects which are only partially resolved, the fitting of such simple functional forms to interferometer data gives a good estimate of the overall size, and permits quantitative comparison with models. Furthermore, this allows sizes for morphologically complex objects Q 2 and Q 3 to be compared against measurements of the partially-resolved Q 1, Q 4 and Q 9, and against other dusty Wolf-Rayets observed with high resolution techniques. Note also that FWHM in the range 10–15 mas are only marginally resolved with this experiment; relative errors in these cases are correspondingly high.

Apparent sizes have been combined with flux measurements to yield estimates of surface brightness in our two filter bandpasses for the target stars. Correction for the A_v=29±5 visible extinction was made using the optical dust constants of Mathis(4). Surface brightnesses were then derived following Monnier et al.(6), which also gives a comparison population of Galactic dusty Wolf-Rayets with similarly measured surface brightnesses. For both filter bandpasses, the Quintuplet cocoon stars showed surface brightnesses within the range spanned by the WR population studied in Monnier et al.(6). In particular, for Q4 and Q9 the color temperature between 2.21 and 3.08 μm appeared to be in reasonable accord with similar measurements from the Galactic population. This finding was found to be generally robust against variations in the extinction correction over the expected range.

However, in some regards the Quintuplet WRs, and in particular Q 2 and Q 3, did appear to be distinct from the Galactic population. The observed increase in size between 2.21 and 3.08 μm which approaches a factor of ∼2 in the Quintuplet, is found to be a more modest ∼1.4 elsewhere(9; 6). Such changes of size (and surface brightness) with wavelength reflect the fact that dust with a range of temperatures contributes to the near-IR emission. The dramatic enlargement between 2.21 and 3.08 μm argues for a flatter thermal profile in the Quintuplet dust shells: plausibly due to external heating from stars in the dense central region of the cluster. The comparison population of Galactic WRs were in far less crowded regions where the outer dust shell likely receives little or no energy except that originating with the central WR star.

Perhaps the simplest way to test the hypothesis that the remaining 3 cocoon stars are also pinwheels is by photometric monitoring. Variability of these sources has already been noted(2), although not with sufficient coverage to reveal a cyclic change consummate with any rotational period(3). The $\sim$2.5 yr periods inferred from the imaging extend the confirmed operation of continuous dust formation by the pinwheel mechanism to significantly longer periods/larger binary separations than previously known, with implications for models of these processes.

This finding of late-type WC binaries in the Quintuplet means that WC (Carbon rich) outnumber WN (Nitrogen rich) Wolf-Rayets by 11:6, and furthermore all WC stars are dusty. This makes an interesting contrast to the massive young WR-rich cluster Westerlund 1 where the WC:WN ratio is reversed to 7:12, with none of the WC's exhibiting dust. Clearly, the close binaries at the heart of the Pinwheel systems can be responsible for significant modification of the stellar evolutionary path, in which mass-transfer or envelope-stripping events might precipitate the WC phase. This entanglement of binarity, mass-loss history, and evolutionary path has the potential to skew population distributions, although it is unclear exactly what conditions resulted in the abundance of Pinwheels in this cluster.

REFERENCES

1 Figer, D. F., Kim, S. S., Morris, M., Serabyn, E., Rich, R. M., & McLean, I. S. 1999, ApJ, 525, 750

2 Glass, I. S., Matsumoto, S., Carter, B. S., & Sekiguchi, K. 2002, MNRAS, 336, 1390

3 Kato, T., Haseda, K., Yamaoka, H., & Takamizawa, K. 2002, PASJ, 54, L51

4 Mathis, J. S. 1990, ARA&A, 28, 37

5 Moneti, A., Glass, I. S., & Moorwood, A. F. M. 1994, MNRAS, 268, 194

6 Monnier, J. D., Tuthill, P. G., Danchi, W. C., Murphy, N. M., & Harries, T. J. 2006, ApJ, Submitted

7 Okuda, H., et al. 1990, ApJ, 351, 89

8 Tuthill, P. G., Monnier, J. D., Danchi, W. C., Wishnow, E. H., & Haniff, C. A. 2000, PASP, 112, 555

9 Tuthill, P. G., Monnier, J. D., & Danchi, W. C. 2002, ASP Conf. Ser. 260: Interacting Winds from Massive Stars, 260, 321

This manuscript was prepared with the AAS LaTeX macros v5.0.

Table S1. Observing long and apparent sizes

Source(5)	Alt. Name(7)	Date	2.21 μm FWHM (mas)	3.08 μm FWHM (mas)
Q 1	GCS 3-4	1998 Aug 06	18±3	–
Q 2	GCS 3-2	1998 Aug 06	35±2	–
		1999 May 04	38±3	–
		1999 Jul 29	37±3	77±2
Q 3	GCS 4	1998 Aug 06	41±2	–
		1999 Jul 29	40±2	75±2
Q 4	GCS 3-1	1998 Aug 06	13±4	–
		2002 Jul 23	15±3	20±3
Q 9	GCS 3-3	1998 Aug 06	13±4	–
		2002 Jul 23	< 11	21±3

Note. — Log of observations of the five cocoon stars. Observations in the K band at 2.21 μm were made at all epochs, but longer wavelength data at 3.08 μm were only secured on the four occasions listed. The FWHM of a circular Gaussian profile fit to the visibility data is also given, together with the estimated uncertainty, as a measure of the overall apparent size.

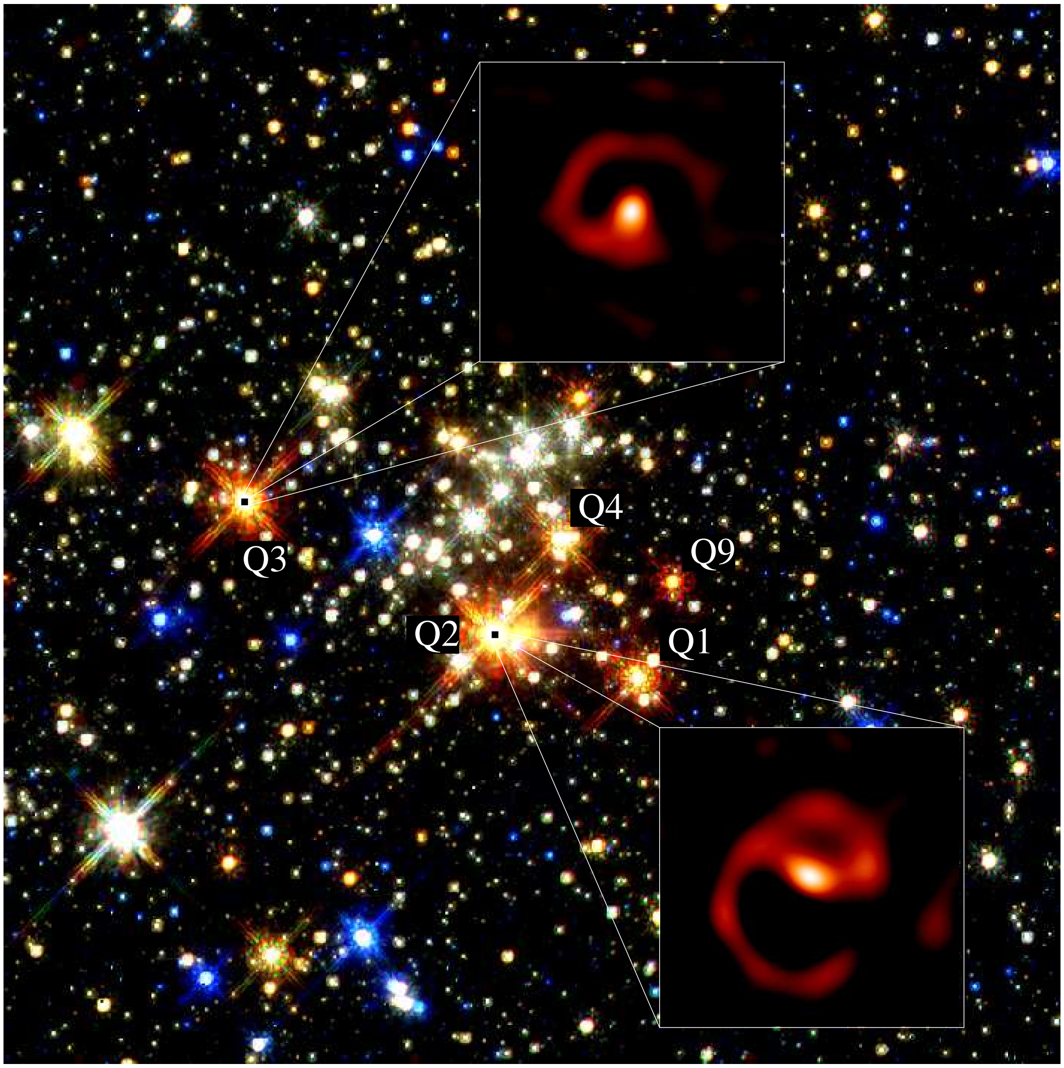

Fig. S1– The background star-field is from multi-wavelength Hubble Space Telescope (NICMOS) near-infrared imaging. Further details and discussion of this image can be found in Figer et al. (1). The five dusty red cocoon stars are labelled according to the nomenclature of Moneti et al. (5). Inset images of Q 2 and Q 3 recovered with our Keck imaging experiments (see also Fig. 1) are overlayed, with graphical indication showing the relative scaling between the Hubble and Keck imaging.